# Synthesis, Structure, Spectroscopic Properties, and Electrochemistry of Rare Earth Sandwich Compounds with Mixed 2,3-Naphthalocyaninato and Octaethylporphyrinato Ligands

**Jianzhuang Jiang,*[a] Yongzhong Bian,[a] Fumio Furuya,[b] Wei Liu,[a, c] Michael T. M. Choi,[c] Nagao Kobayashi,*[b] Hung-Wing Li,[c] Qingchuan Yang,[c] Thomas C. W. Mak,[c] and Dennis K. P. Ng*[c]**

**Abstract:** A series of 14 heteroleptic rare earth sandwich complexes [$M^{III}$(nc)(oep)] (M = Y, La–Lu except Ce and Pm; nc = 2,3-naphthalocyaninate; oep = octaethylporphyrinate) have been prepared by a one-pot procedure from the corresponding [M(acac)$_3$]·$n$H$_2$O (acac = acetylacetonate), metal-free porphyrin H$_2$(oep), and naphthalonitrile in the presence of 1,8-diazabicyclo[5.4.0]undec-7-ene (DBU) in *n*-octanol. The molecular structures of four of these complexes (M = Sm, Gd, Y, Lu) are isostructural, exhibiting a slightly distorted square antiprismatic geometry with two domed ligands. The interplanar distance decreases from 2.823 to 2.646 Å along the series as a result of lanthanide contraction. The whole series of complexes have also been characterized spectroscopically. All the electronic absorptions, except the two B-bands due to nc and the oep rings, are metal-dependent, indicating that there are substantial $\pi-\pi$ interactions. The hole or the unpaired electron in these double-deckers is delocalized over both macrocyclic ligands, as evidenced by the co-appearance of the IR marker bands for the nc$^{\bullet-}$ (1315–1325 cm$^{-1}$) and oep$^{\bullet-}$ (1510–1531 cm$^{-1}$) $\pi$ radical ions. Three one-electron oxidation couples and up to three one-electron reduction couples have been revealed by electrochemical methods. All the potentials are linearly dependent on the size of the metal center. The changes in absorption spectra during the first electro-oxidation and reduction of the $La^{III}$, $Eu^{III}$, and $Y^{III}$ double-deckers have also been studied spectroelectrochemically. The spectral data recorded for [$M^{III}$(nc)(oep)]$^-$ (M = Y, La–Lu except Ce and Pm) reduced chemically with hydrazine hydrate are in accord with those obtained by spectroelectrochemical methods. The first heteroleptic naphthalocyaninate-containing triple-deckers [$M^{III}_2$(nc)(oep)$_2$] (M = Nd, Eu) have also been prepared by a raise-by-one-story method by using [$M^{III}$(nc)(oep)] (M = Nd, Eu), [M(acac)$_3$]·$n$H$_2$O (M = Nd, Eu), and H$_2$(oep) as starting materials. The compounds adopt a symmetrical triple-decker structure with two outer oep rings and one inner nc ring, which has been confirmed by $^1$H NMR spectroscopy and X-ray structural determination of the Nd complex. Both compounds give a near-IR absorption at 1021 nm (for M = Nd) or 1101 nm (for M = Eu), which has rarely been observed for neutral (or hole-free) triple-decker complexes and can be ascribed to the lowest-energy Q′(0, 0) transition. Similarly to the double-decker analogues, these triple-decker complexes undergo a series of one-electron transfer processes with a relatively small potential gap (1.1–1.2 V) between the first oxidation and the first reduction.

**Keywords:** lanthanides · phthalocyanines · pi interactions · porphyrins · sandwich complexes

## Introduction

Phthalocyanines and porphyrins are important classes of pigments that have applications in various disciplines.[1, 2] Both series belong to a cyclic tetrapyrrole family in which the four isoindole or pyrrole nitrogen atoms can form complexes with a range of metal ions. With large metal centers that favor octacoordination (for example, rare earths, actinides, Group 4

[a] Prof. J. Jiang, Y. Bian, W. Liu
Department of Chemistry, Shandong University
Jinan 250100 (China)
Fax: (+86)531-856-5211
E-mail: jzjiang@sdu.edu.cn

[b] Prof. N. Kobayashi, F. Furuya
Department of Chemistry, Graduate School of Science
Tohoku University, Sendai 980-8578 (Japan)
Fax: (+81)22-217-9279
E-mail: nagaok@mail.cc.tohoku.ac.jp

[c] Prof. D. K. P. Ng, W. Liu, M. T. M. Choi, H.-W. Li, Prof. Q. Yang, Prof. T. C. W. Mak
Department of Chemistry
The Chinese University of Hong Kong
Shatin, N.T., Hong Kong (China)
Fax: (+852)2603-5057
E-mail: dkpn@cuhk.edu.hk

Supporting information for this article is available on the WWW under http://wiley-vch.de/home/chemistry/ or from the authors.

  0947-6539/01/0723-5059 $ 17.50+.50/0 

transition metals, and main group elements such as In, Sn, As, Sb, and Bi), sandwich-type complexes in the form of double- (A) and triple-deckers (B) can be formed (Figure 1).[3] Because of the intramolecular $\pi-\pi$ interactions and the intrinsic nature of the metal centers, these novel complexes display characteristic features that cannot be found in their non-sandwich counterparts and which enable them to be used in different areas. Bis(phthalocyaninato)lanthanide(III) complexes, for example, are versatile materials for electrochromic displays,[4] field-effect transistors,[5] and gas sensors.[6] The bis(porphyrinato)cerium(IV) analogues have been put forward as structural and spectroscopic models for the special pair found in bacterial photosynthetic reaction centers.[7] Recently, these complexes have also been used for chirality transcription, as saccharide receptors through positive homotropic allosterism,[8] and as redox-responsive rotating modules.[9] Homoleptic sandwich complexes containing the same tetrapyrrole ligands have been studied extensively, but relatively little is known about the heteroleptic counterparts (Figure 1), partly because of the synthetic barrier and the difficulty of isolation and purification.[3, 10]

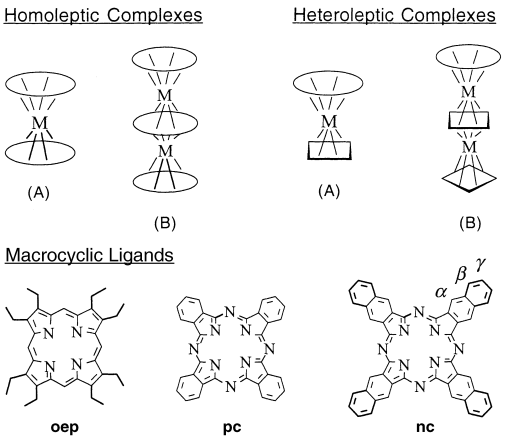


Figure 1. Schematic structures of homoleptic and heteroleptic sandwich complexes with tetrapyrrole ligands.

For sandwich complexes with an unpaired electron in one of the tetrapyrrole ligands, a fundamental question concerns the extent of hole delocalization. It has been found by spectroscopic methods that for $[M^{III}(pc)(tpp)]$ (M = Y, La, Pr, Nd, Eu, Gd, Er, Lu),[11, 12] $[Eu^{III}(oep)(tpp)]$,[13] and $[M^{IV}(oep)(tpp)]^+$ (M = Ce,[14] Th[15]), the hole resides mainly on the pc or the oep rings, which is consistent with the lower oxidation potentials of these macrocycles compared with that of tpp. For the cationic complexes $[M^{IV}(oep)(pc)]^+$ (M = Zr, Hf, Th, U),[16] there is substantial evidence that the hole is delocalized over both macrocycles. To improve understanding of this issue, more examples are needed of heteroleptic complexes in which the individual chromophoric ligands exhibit very different optical and redox properties.

2,3-Naphthalocyanine has a more extended $\pi$ system. As shown experimentally and by theoretical calculations,[17] the linear benzoannulation destabilizes the HOMO level leading to a smaller HOMO–LUMO gap. As a result, 2,3-naphthalocyanine has a lower ionization energy and oxidation potential than the phthalocyanine analogue, and its characteristic Q-band is also significantly red-shifted. Similar results have also been found for the double-decker complexes $[Lu^{III}(nc)_2]$[11, 18] and $[M^{III}\{nc(t\mathrm{Bu})_4\}_2]$ (M = Y, La–Nd, Eu–Tb, Er),[19] which have the narrowest HOMO–LUMO gaps (0.28–0.33 V determined by cyclic voltammetry) ever reported for this kind of complex.

Although naphthalocyaninate-containing sandwich compounds have been known for some time, studies have been focused on the homoleptic complexes, mainly of lutetium(III).[18, 20] Heteroleptic naphthalocyaninato complexes remain extremely rare.[21] Recently, we briefly reported on some of these complexes: $[Eu^{III}(nc)(tpyp)]$,[11, 22] $[Eu^{III}\{nc(SC_{12}H_{25})_8\}(tpyp)]$,[22] $[Eu^{III}\{nc(t\mathrm{Bu})_4\}(tClpp)]$,[23] and $[M^{III}(nc)(tbpp)]$ (M = Y, La–Tm except Ce and Pm).[23] In this paper, we report a more detailed and systematic investigation of the new series of complexes $[M^{III}(nc)(oep)]$ (M = Y, La–Lu except Ce and Pm) and $[M^{III}_2(nc)(oep)_2]$ (M = Nd, Eu), including the first structural characterization of naphthalocyaninato sandwich complexes and the first naphthalocyaninate-containing mixed triple-deckers.

## Results and Discussion

**Synthesis of $[M^{III}(nc)(oep)]$ and $[M^{III}_2(nc)(oep)_2]$**: Among several synthetic pathways to lanthanide(III) double-decker complexes with mixed tetrapyrrole ligands $[M^{III}(ring\text{-}1)(ring\text{-}2)]$,[3, 10] the most commonly used involves prior generation of the half-sandwich complexes [M(acac)(ring-1)] from $[M(acac)_3]\cdot nH_2O$ and $H_2$(ring-1) or $Li_2$(ring-1), followed by treatment with $H_2$(ring-2), $Li_2$(ring-2), or the (na)phthalocyanine precursors, (na)phthalonitriles (for ring-2 = pc or nc derivatives). We found that this stepwise raise-by-one-story reaction could be simplified to a one-pot procedure. Thus treatment of $[M(acac)_3]\cdot nH_2O$ (M = Y, La–Lu except Ce and Pm) with $H_2$(oep) and naphthalonitrile in the presence of DBU in *n*-octanol led to the formation of the corresponding $[M^{III}(nc)(oep)]$ (**1**–**14**) in 21–45% yield (Scheme 1).[24] It has been found that for the lanthanide(III) complexes $[M^{III}(oep)_2]$ and $[M^{III}\{nc(t\mathrm{Bu})_4\}_2]$,[19a, 25] the yield of the double-deckers diminishes progressively with the size of the central metal ion as a result of an increase in axial compression of the two macrocyclic ligands. Similar results were observed for **2**–**14**, but the effect of metal on the reaction yield was slightly smaller for this series of complexes. The lanthanum complex $[La^{III}(nc)(oep)]$ (**1**) appeared to be less stable than the other double-deckers; it decomposed slowly during chromatography giving a trace amount of $H_2$(oep) as a red fraction in front of the major band of **1** at every stage of chromatographic purification. Presumably, the ring-to-ring separation is slightly too great in this complex to allow sufficient interactions between the macrocycles to stabilize the sandwich-type system.

The first nc-containing heteroleptic triple-decker complexes $[M^{III}_2(nc)(oep)_2]$ [M = Nd (**15**) and Eu (**16**)] were



0947-6539/01/0723-5060 $ 17.50+.50/0 *Chem. Eur. J.* **2001**, *7*, No. 23

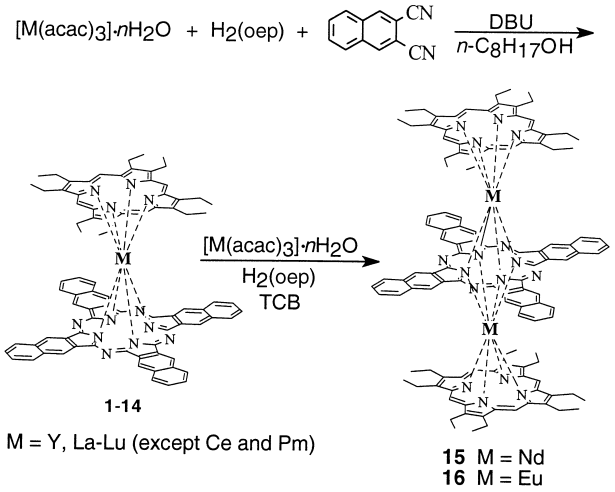


Scheme 1. Synthesis of double- and triple-decker complexes.

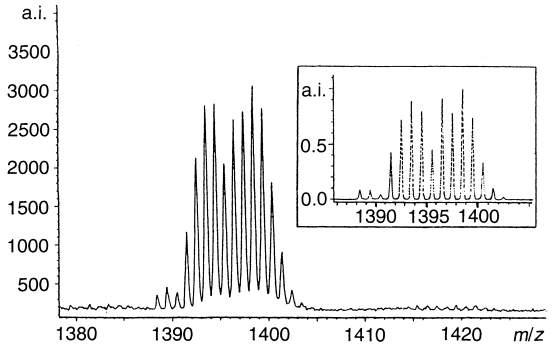


Figure 2. Partial MALDI-TOF mass spectrum of [$Sm^{III}$(nc)(oep)] (**4**) showing the isotopic distribution of the molecular ion. Inset: the corresponding simulated pattern.

prepared by repeating the raise-by-one-story reaction by using [$M^{III}$(nc)(oep)] [M = Nd (**3**), Eu (**5**)] as starting materials. Treatment of these double-deckers with $H_2$(oep) and [$M(acac)_3$]·$nH_2O$ (M = Nd, Eu) in refluxing 1,2,4-trichlorobenzene (TCB) gave the triple-deckers **15** and **16** (Scheme 1). This method is similar to that employed by Weiss et al., who prepared the mixed-metal triple-deckers [(tpp)$M^1$(pc)$M^2$(por)] ($M^1$ = La, Ce; $M^2$ = Y, Gd, Lu; por = oep, tpp) by treating [$M^1$(pc)(tpp)] with [$M^2$(acac)(por)].[26] Again, the prior generation of [M(acac)(por)] was found to be unnecessary in the preparation of **15** and **16**.[27]

**Spectroscopic characterization**: All the new compounds were fully characterized by elemental analyses and various spectroscopic methods. Mass spectrometry is a powerful technique for characterizing this class of compounds as some of the lanthanides give very distinct isotopic patterns.[28] The MALDI-TOF mass spectrum of [$Sm^{III}$(nc)(oep)] (**4**; Figure 2) is an example. The good agreement of the relative abundance of the isotopic cluster with the simulated spectrum of $[Sm(nc)(oep)]^+$ (inset) provides strong evidence for the identity of this compound.

Like other lanthanide(III) bis(tetrapyrrole) complexes,[3, 10] **1**–**14** can be regarded as single-hole complexes in which one of the macrocyclic ligands contains an unpaired electron. This was confirmed by the EPR spectra of [$M^{III}$(nc)(oep)] (M = La (**1**), Y (**9**), Lu (**14**)). The spectra recorded in $CH_2Cl_2$ at ambient temperature showed a sharp signal at $g = 1.9999 - 2.0020$ with a linewidth of 5.4–10.3 G, which is typical of organic radicals. All the remaining double-deckers were EPR-silent under these conditions, probably because of the paramagnetic nature of the metal centers.

Due to the presence of the unpaired electron and the paramagnetic nature of some of the lanthanide ions, NMR data for these complexes are difficult to obtain. However, upon addition of hydrazine hydrate as a reducing agent,[18, 29] satisfactory $^1$H NMR spectra could be obtained for the reduced form of [$M^{III}$(nc)(oep)] (M = La (**1**), Eu (**5**), Y (**9**), Lu (**14**)), in which both of the macrocycles become diamagnetic (i.e. [$M^{III}(nc^{2-})(oep^{2-})]^-$).[30] The NMR spectra for the reduced complexes **1**, **9**, and **14**, which have a closed-shell metal center, were very similar, with a singlet at $\delta = 9.58 - 9.60$ and two well-resolved doublets of doublets at $\delta = 8.73 - 8.76$ and 7.91–7.94 for the $\alpha$, $\beta$, and $\gamma$ ring protons of the nc ligand, respectively. The oep proton signals appeared at $\delta = 8.81 - 8.92$ (s, *meso*-H) and 1.76–1.90 (t, $CH_3$), while the methylene proton signals were obscured by the strong water signal at $\delta \approx 3.5$ (Table 1). Having a paramagnetic $Eu^{III}$ center, the reduced **5** gave a similar $^1$H NMR spectrum with signals spreading to a wider region (Table 1). The singlet for the oep *meso*-protons appeared at a more downfield position ($\delta = 15.04$), and two multiplets for the diastereotopic methylene protons (at $\delta \approx 5.6, 4.4$) could be observed in this case.[31]

The triple-deckers **15** and **16** contain three diamagnetic dianionic macrocyclic ligands, so they can be characterized by NMR spectroscopy even in the absence of hydrazine hydrate. The $^1$H NMR spectra of these compounds included only four sets of aromatic signals in a 1:1:1:1 ratio, showing that the triple-deckers adopt a symmetrical [(oep)M(nc)M(oep)]

Table 1. $^1$H NMR data ($\delta$) for the reduced form of the double-deckers **1**, **5**, **9**, and **14**.[a]

| | nc | | | oep | | |
|---|---|---|---|---|---|---|
| | nc-$H_\alpha$ | nc-$H_\beta$ | nc-$H_\gamma$ | *meso*-H | $CH_2$ | $CH_3$ |
| [La(nc)(oep)] (**1**) | 9.60 (s) | 8.76 (dd, $J = 3.2, 6.1$ Hz) | 7.94 (dd, $J = 3.2, 6.1$ Hz) | 8.92 (s) | 3.65–3.70 (m)[b] | 1.90 (t, $J = 7.2$ Hz) |
| [Eu(nc)(oep)] (**5**) | 10.98 (s) | 9.42 (dd, $J = 2.9, 6.1$ Hz) | 8.27 (dd, $J = 2.9, 6.1$ Hz) | 15.04 (s) | 5.56–5.61 (m)4.41–4.47 (m) | 3.00 (t, $J = 7.3$ Hz) |
| [Y(nc)(oep)] (**9**) | 9.58 (s) | 8.73 (dd, $J = 3.2, 6.1$ Hz) | 7.91 (dd, $J = 3.2, 6.1$ Hz) | 8.82 (s) | –[c] | 1.80 (t, $J = 7.6$ Hz) |
| [Lu(nc)(oep)] (**14**)[d] | 9.58 (s) | 8.73 (dd, $J = 3.2, 6.3$ Hz) | 7.94 (dd, $J = 3.2, 6.3$ Hz) | 8.81 (s) | –[c] | 1.76 (t, $J = 7.7$ Hz) |

[a] Recorded in [$D_7$]DMF with the addition of 1% hydrazine hydrate on a 400 MHz spectrometer unless otherwise stated. [b] The other set of methylene proton signals is embedded in the strong band of water at $\delta \approx 3.5$. [c] The signals are obscured by the strong signal of water at $\delta \approx 3.5$. [d] Recorded on a 300 MHz spectrometer.

structure in which the two oep rings are related by symmetry. Similarly to the double-decker analogue $[Eu(nc)(oep)]^-$, two multiplets were also observed for the two sets of diastereotopic methylene protons of the oep rings.

The absorption spectral data of the sandwich compounds **1**–**16** recorded in $CHCl_3$ are compiled in Table 2. The dependence of the spectral features of the double-deckers on the metal is illustrated with the spectra of $[M^{III}(nc)(oep)]$ [M = Pr (**2**), Yb (**13**)] (Figure 3), which show strong nc and

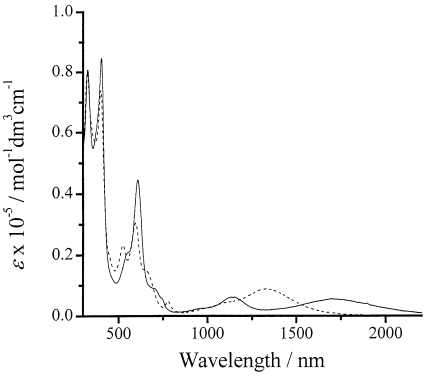


Figure 3. Electronic absorption spectra of $[Pr^{III}(nc)(oep)]$ (**2**) (——) and $[Yb^{III}(nc)(oep)]$ (**13**) (– – –) in $CHCl_3$.

oep B-bands (or Soret bands) at approximately 325 and 400 nm, respectively. The former is very close to the pc B-band observed in the spectra of $[M^{III}(pc)(por)]$ (por = *meso*-tetraarylporphyrinate) with a higher intensity.[12, 32] Three visible bands (607, 703, and 743 nm for **2**, and 595, 655, and 778 nm for **13**) can be ascribed to the Q-bands of the macrocycles. These signals are well resolved for complexes with a smaller metal center, but some of them appear as shoulders as the size of the metal center increases (Figure 3). The absorption positions of these bands are also dependent on the ionic radius of the metal center. When the metal center becomes smaller, the longest-wavelength visible band (743–779 nm) shifts gradually to the red, while the other two absorptions are blue-shifted (Table 2). Interestingly, these Q-bands are almost invisible for the pc analogues $[M^{III}(pc)(por)]$.[12, 32]

By analogy with the double-deckers $[M^{III}(pc)(por)]$,[12, 32] the visible band at 522–554 nm and the near-IR absorption at 1091–1336 nm for **1**–**14** may arise from a hole localized on the nc ring. Since such characteristic π–radical-anion bands can also be observed for $[M^{III}(oep)_2]$ at approximately 540 and 670 nm,[33] the 540 nm band may also have a contribution from the $oep^{\bullet-}$. Owing to the extension of the π-conjugated system, these two bands are substantially red-shifted compared with those of $[M^{III}(pc)(tpp)]$ (468–484 and 965–1067 nm),[12b] but the similarity in their trends of metal dependence provides additional support for the assignment.

For the double-deckers $[M^{III}(nc)(oep)]$ (M = La–Dy), which have larger metal centers, an additional near-IR band at 1463–1816 nm can also be seen (Table 2 and Figure 3). According to the "supermolecular" molecular orbital model,[34] this signal, which is highly characteristic for single-hole complexes, can be attributed to an electronic transition from the second-highest-filled supermolecular bonding orbital to the half-filled supermolecular antibonding orbital.[35] Similarly to $[M^{III}(pc)(tpp)]$,[12b] this band undergoes a hypsochromic shift as the ionic radius of the metal center decreases. For the rest of the series (**9**–**14**), this signal cannot be observed. It is likely that as the size of the metal center decreases, the separation between the two near-IR bands becomes smaller and eventually the two bands coalesce to form a single broad signal (Table 2). All the visible and near-IR bands in the spectra of $[M^{III}(nc)(oep)]$ (**1**–**14**) vary systematically with the ionic radius of the metal center. This strongly suggests that significant π–π interactions are present in these double-decker complexes.

The absorption spectrum (Figure 4) of the triple-decker $[Nd^{III}_2(nc)(oep)_2]$ (**15**) is very similar to that of the Eu analogue **16**. The nc B-band for these two complexes (337–352 nm) is split into two partially resolved signals of equal intensity, while the oep B-band (406–407 nm) remains sharp and intense. The spectra also display several relatively weak absorptions that can be attributed to the Q-band transitions. Interestingly, one of these signals extends to the near-IR region (1021 nm for **15** and 1101 nm for **16**) (Table 2). By

Table 2. UV/Vis and near-IR spectroscopic data for **1**–**16** in $CHCl_3$.

| | $\lambda_{max}$ [nm] (log ε) | | | | | | | |
|---|---|---|---|---|---|---|---|---|
| [La(nc)(oep)] (**1**) | 327 (4.73) | 404 (4.80) | 554 (sh) | 612 (4.48) | 712 (sh) | 745 (sh) | 1091 (3.62) | 1816 (3.46) |
| [Pr(nc)(oep)] (**2**) | 327 (4.91) | 402 (4.92) | 547 (sh) | 607 (4.65) | 703 (sh) | 743 (sh) | 1139 (3.79) | 1719 (3.72) |
| [Nd(nc)(oep)] (**3**) | 327 (4.94) | 403 (4.94) | 545 (sh) | 605 (4.66) | 686 (4.07) | 749 (sh) | 1157 (3.81) | 1642 (3.76) |
| [Sm(nc)(oep)] (**4**) | 328 (5.04) | 401 (4.98) | 540 (sh) | 603 (4.78) | 694 (sh) | 752 (sh) | 1189 (3.98) | 1561 (3.83) |
| [Eu(nc)(oep)] (**5**) | 326 (4.98) | 401 (4.89) | 539 (4.36) | 601 (4.68) | 684 (sh) | 757 (sh) | 1196 (3.85) | 1542 (3.76) |
| [Gd(nc)(oep)] (**6**) | 327 (5.04) | 400 (4.98) | 536 (4.47) | 600 (4.76) | 677 (sh) | 754 (sh) | 1208 (3.97) | 1522 (3.87) |
| [Tb(nc)(oep)] (**7**) | 326 (5.05) | 400 (4.99) | 535 (4.47) | 598 (4.74) | 676 (sh) | 760 (sh) | 1223 (3.92) | 1480 (3.87) |
| [Dy(nc)(oep)] (**8**) | 325 (4.97) | 399 (4.93) | 530 (4.42) | 597 (4.63) | 668 (4.19) | 766 (3.64) | 1251 (3.90) | 1463 (3.86) |
| [Y(nc)(oep)] (**9**) | 327 (4.99) | 399 (4.93) | 530 (4.23) | 596 (4.67) | 658 (sh) | 772 (3.80) | 1308 (4.11) | |
| [Ho(nc)(oep)] (**10**) | 325 (5.10) | 400 (5.06) | 528 (4.57) | 597 (4.76) | 662 (4.35) | 771 (3.83) | 1287 (4.06) | |
| [Er(nc)(oep)] (**11**) | 324 (5.11) | 399 (5.07) | 525 (4.58) | 595 (4.75) | 658 (4.37) | 772 (3.80) | 1319 (4.11) | |
| [Tm(nc)(oep)] (**12**) | 324 (4.95) | 398 (4.90) | 525 (4.42) | 594 (4.58) | 657 (4.21) | 775 (3.64) | 1328 (3.97) | |
| [Yb(nc)(oep)] (**13**) | 324 (4.90) | 400 (4.87) | 524 (4.37) | 595 (4.48) | 655 (4.18) | 778 (3.68) | 1331 (3.95) | |
| [Lu(nc)(oep)] (**14**) | 324 (4.93) | 398 (4.85) | 522 (4.37) | 591 (4.51) | 654 (4.15) | 779 (3.57) | 1336 (3.89) | |
| $[Nd_2(nc)(oep)_2]$ (**15**) | 337 (5.18) | 352 (5.17) | 407 (5.41) | 524 (4.39) | 637 (4.41) | 1021 (4.27) | | |
| $[Eu_2(nc)(oep)_2]$ (**16**) | 338 (5.08) | 350 (5.07) | 406 (5.22) | 525 (4.21) | 640 (4.41) | 1101 (3.93) | | |



0947-6539/01/0723-5062 $ 17.50+.50/0 *Chem. Eur. J.* **2001**, *7*, No. 23

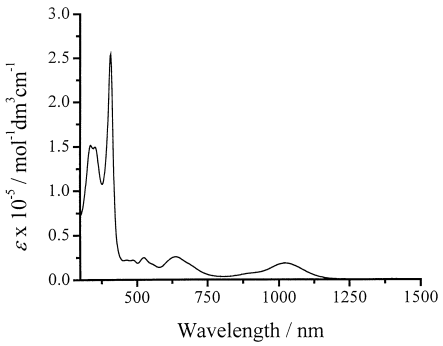


Figure 4. Electronic absorption spectrum of $[Nd^{III}_2(nc)(oep)_2]$ (**15**) in $CHCl_3$.

analogy with the proposed origin of the Q′ state of the triple-deckers $[M^{III}_2(oep)_3]$ (600–800 nm), which is believed to be associated primarily with configurations arising from the one-electron transitions from the top (antibonding) HOMOs to the lowest (bonding) LUMOs,[36] this near-IR transition may be ascribed to the lowest-energy Q′(0, 0)-band. The assignment is supported by the electrochemical data and the spectral properties of the related anionic double-deckers $[M^{III}(nc)(oep)]^-$ (M = Y, La–Lu except Ce and Pm), which also contain only dianionic macrocyclic ligands (see below). Near-IR bands are usually associated with an unpaired electron or hole in sandwich-type complexes.[3, 10] The results for **15** and **16** show that electronic transitions may also appear in the near-IR region for sandwich compounds with only dianionic ligands. Re-examination of the absorption spectra of the heteroleptic triple-deckers $[M^{III}_2(pc)(por)_2]$ showed that the compounds do exhibit a near-IR absorption at approximately 860–980 nm[37] which had been ignored in most of the previous studies.[26, 38, 39]

According to the electronic absorption spectra, it appears that the hole in the double-deckers **1**–**14** is delocalized on the electronic timescale ($10^{-15}$ s). The co-existence of $nc^{\bullet-}$ and $oep^{\bullet-}$ character in the complexes was also revealed by IR spectroscopy, which along with Raman spectroscopy is a versatile tool for probing the extent of hole delocalization in these sandwich-type complexes.[40] There were IR marker bands for these π radical anions at 1315–1325 (medium to strong) and 1510–1531 $cm^{-1}$ (weak to medium);[16, 19, 22, 23] this shows that the hole or the unpaired electron resides on a mixed nc/oep orbital. This can be rationalized in terms of the similar oxidation potentials of related nc and oep complexes.[41] Similarly, diagnostic bands belonging to both $oep^{\bullet-}$ (1515–1547 $cm^{-1}$) and $pc^{\bullet-}$ (1310–1321 $cm^{-1}$) were observed[16] for the cationic single-hole complexes $[M^{IV}(oep)(pc)]^+$ (M = Zr, Hf, Th, U). As expected, the characteristic IR marker bands for $nc^{\bullet-}$ and $oep^{\bullet-}$ π radical anions were not observed for the triple-deckers **15** and **16**, which contain only dianionic macrocyclic ligands. However, both spectra showed three moderately strong absorptions at 1308–1361 $cm^{-1}$ which, by analogy with the pc counterparts,[40a] are believed to be the marker bands for $nc^{2-}$.

**Structural studies**: The molecular structures of **4**, **6**, **9**, **14**, and **15** were also determined by single-crystal X-ray analyses. Although nc-containing sandwich complexes are known,[18–23] structural data of this class of compounds have not been reported so far. The single crystals were grown by slow diffusion of hexane into their $CHCl_3$ solutions.[42] The structures of **4** and **9** also contained solvated cyclohexane, which may come from the solvents used for crystallization.[43] All the double-deckers have similar structures (Table 3). The structural features of these complexes are exemplified by the molecular structure of $[Y^{III}(nc)(oep)]$ (**9**) (Figure 5). The yttrium center is coordinated by eight nitrogen atoms from the isoindole and pyrrole of the nc and oep rings, respectively, forming a nearly perfect square antiprism with a ring-to-ring separation of 2.700 Å (as defined by the two $N_4$ mean planes). The metal center lies closer to the $N_4$ plane of oep by 0.221 Å, probably because of the larger cavity of oep. The two $N_4$ planes are virtually parallel (dihedral angle 0.6°), but the two ligands are significantly domed. The average dihedral angle ($\varphi$) of the individual isoindole or pyrrole rings with respect to the corresponding $N_4$ mean plane is 14.0° for the nc and 15.2° for the oep ring, showing that the latter is slightly more deformed. The interplanar separation and the average M–N distances decrease with the size of the metal center (Table 3), while the extent of ligand deformation remains essentially unchanged. The average twist angle, defined as the rotation angle of one ring away from the eclipsed conformation of the two rings, or simply the dihedral angle N(nc)–center(nc $N_4$ plane)–center(oep $N_4$ plane)–N(oep), is close to 45° for all these complexes, an indication that the two ligands are almost fully staggered. Ohashi and coworkers have recently reported the structures of a series of bis(phthalocyaninato)lanthanide(III) complexes $[Bu_4N][M(pc)_2]$ (M = Nd, Gd, Ho, Lu).[44] It has been found that the twist (or skew) angle increases from 6.2° to 45.0° as the size of the metal center decreases along the series, suggesting an increase in π–π interactions. Such a trend, however, was

Table 3. Comparison of the structural data for **4**, **6**, **9**, **14**, and **15**.

| | **4** | **6** | **9** | **14** | **15** |
|---|---|---|---|---|---|
| average M–N(nc) bond distance [Å] | 2.507 | 2.473 | 2.456 | 2.439 | 2.711 |
| average M–N(oep) bond distance [Å] | 2.458 | 2.427 | 2.407 | 2.393 | 2.429 |
| M–$N_4$(nc) plane distance [Å] | 1.539 | 1.497 | 1.461 | 1.439 | 1.881 |
| M–$N_4$(oep) plane distance [Å] | 1.285 | 1.256 | 1.240 | 1.207 | 1.274 |
| interplanar distance [Å] | 2.823 | 2.750 | 2.700 | 2.646 | 3.155 |
| dihedral angle between the nc and oep $N_4$ planes [°] | 1.5 | 1.1 | 0.6 | 0.9 | 0.4 |
| average dihedral angle $\varphi$ for the nc ring [°] | 13.0 | 13.2 | 14.0 | 13.1 | 2.6 |
| average dihedral angle $\varphi$ for the oep ring [°] | 15.0 | 15.4 | 15.2 | 14.9 | 9.1 |
| average twist angle [°] | 44.3 | 44.3 | 44.8 | 45.1 | 30.8 |

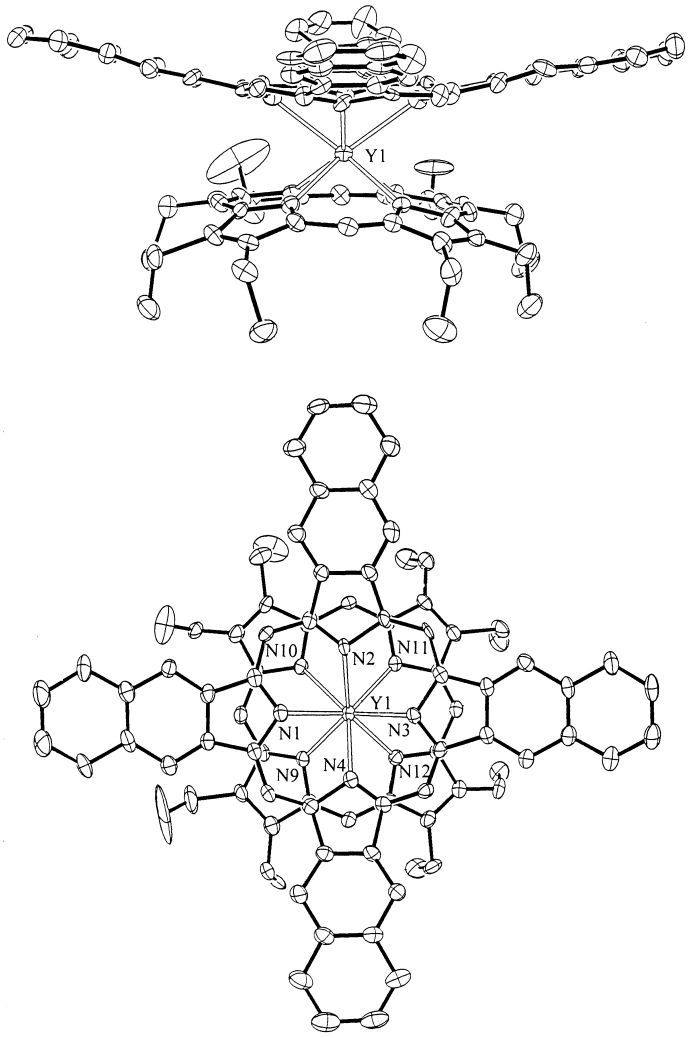


Figure 5. Molecular structure of $[Y^{III}(nc)(oep)]$ (**9**) from two perspectives. Hydrogen atoms are omitted for clarity and the ellipsoids are drawn at 30% probability level.

not observed in the nc/oep heteroleptic double-deckers.[45] It is likely that the staggered orientation can minimize the non-bonding interactions between the fused benzene rings of nc and the $\beta$-ethyl groups of oep.

The triple-decker **15** is centrosymmetric, and the crystal structure contains disordered $CH_2Cl_2$ and water molecules. Each neodymium ion is sandwiched between an outer oep ring and the inner nc ring, giving a symmetrical [(oep)Nd(nc)Nd(oep)] structure (Figure 6), in accord with the NMR data. Each metal center adopts a distorted square antiprismatic geometry with an average twist angle of 30.8°. The inner nc ring is almost planar ($\varphi$ 2.6°), while the outer oep rings are slightly domed toward the metal centers ($\varphi$ 9.1°). The average Nd–N(nc) bond length (2.711 Å) is significantly longer than the average Nd–N(oep) distance (2.429 Å), and the difference (0.282 Å) is much larger than that for the analogous double-deckers (0.046–0.049 Å). The metal centers therefore lie much closer to the oep rings (1.274 compared with 1.881 Å), giving a ring-to-ring separation of 3.155 Å.

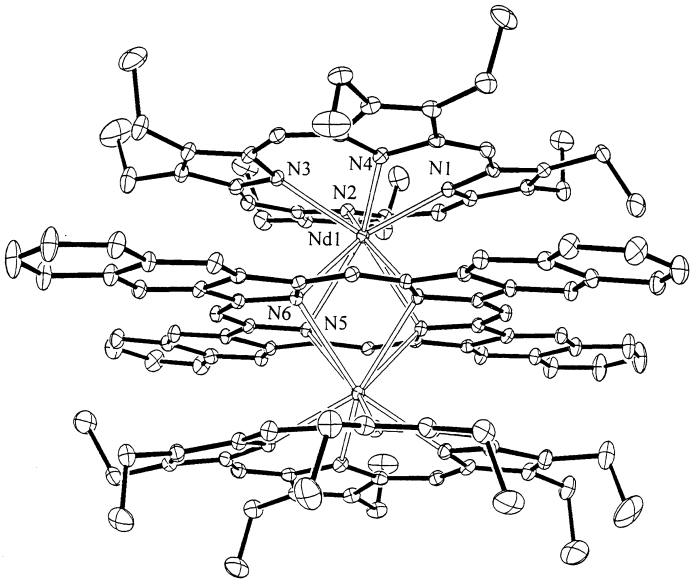


Figure 6. Molecular structure of $[Nd^{III}_2(nc)(oep)_2]$ (**15**) showing the 30% probability thermal ellipsoids for all non-hydrogen atoms.

**Electrochemical properties**: The electrochemical behavior of **1**–**16** was investigated by cyclic voltammetry (CV) and differential pulse voltammetry (DPV) in $CH_2Cl_2$. All the compounds underwent three quasi-reversible one-electron oxidations and two quasi-reversible one-electron reductions. An additional oxidation couple was detected for the triple-deckers **15** and **16**. All these processes can be attributed to successive removal or addition of electrons to the ligand-based orbitals (Scheme 2). Representative cyclic voltammo

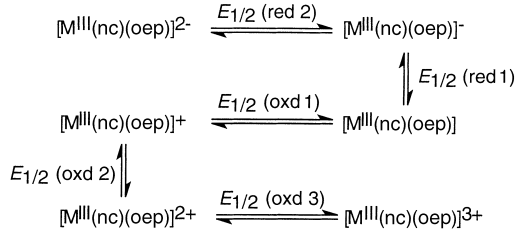


Scheme 2. Different redox states of the double-deckers $[M^{III}(nc)(oep)]$.

grams(for **11** and **16**) are displayed in Figure 7, and the half-wave potentials are summarized in Table 4. Having a more electron-rich oep ligand, complexes **1**–**14** have a lower first oxidation potential (0.19–0.49 V) and a more negative first reduction potential (−0.22–0.06 V) than the corresponding tbpp analogues $[M^{III}(nc)(tbpp)]$ (0.42–0.55 and −0.10–0.05 V, respectively).[23] Figure 8 shows the variation of the redox potentials of **1**–**14** with the ionic radius of the metal center.[46] Similarly to those observed in other series of bis(tetrapyrrole) rare earth(III) complexes,[12b, 19a, 23, 41b, 47] both the first oxidation and the first reduction potentials of **1**–**14** are linearly dependent on the size of the metal center. The gradients (1.42 and 1.30 V Å$^{-1}$, respectively) are more positive than those observed for $[M^{III}(oep)_2]$ (0.91 and 1.24 V Å$^{-1}$)[41b] and $[M^{III}\{nc(tBu)_4\}_2]$ (0.86 and 1.08 V Å$^{-1}$),[19a] showing that the influence of metal size on these potentials (or the HOMO



0947-6539/01/0723-5064 $ 17.50+.50/0 *Chem. Eur. J.* **2001**, *7*, No. 23

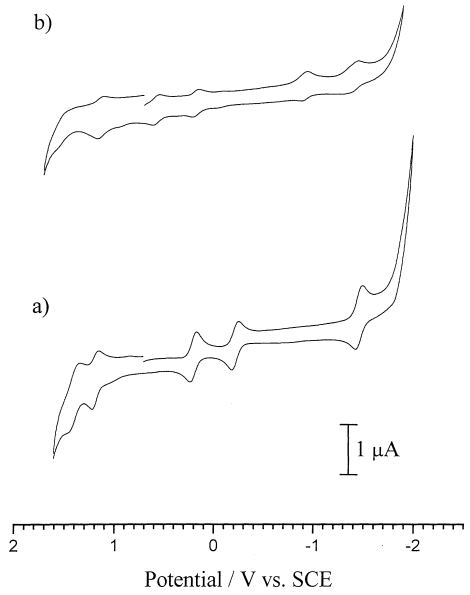


Figure 7. Cyclic voltammograms of a) $[Er^{III}(nc)(oep)]$ (**11**) and b) $[Eu^{III}_2(nc)(oep)_2]$ (**16**) in $CH_2Cl_2$ containing 0.1 mol dm$^{-3}$ $[Bu_4N][PF_6]$ at a scan rate of 100 mV s$^{-1}$.

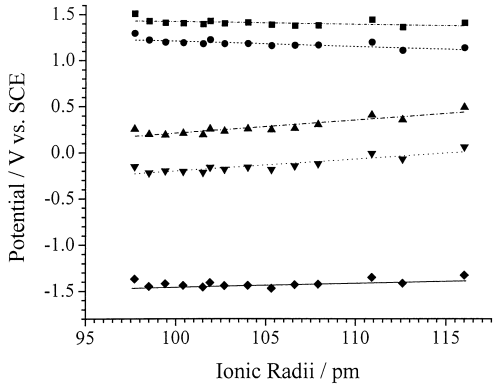


Figure 8. Redox potentials of $[M^{III}(nc)(oep)]$ (**1**–**14**) as a function of the ionic radius of the metal center;[57] ◆ = second reduction, ▼ = first reduction, ▲ = first oxidation, ● = second oxidation, ■ = third oxidation.

and LUMO levels) is greater for the heteroleptic complexes. However, the potential difference between these two processes, which is a measure of the molecular band (or HOMO–LUMO) gap, is rather insensitive to the metal center and ranges from 0.391 to 0.433 V. These values are slightly higher than those of the homoleptic analogues $[M^{III}(oep)_2]$ (0.32–0.365 V)[41b] and $[M^{III}\{nc(tBu)_4\}_2]$ (0.28–0.34 V),[19a] but slightly lower than those of $[M^{III}(pc)_2]$ (0.441–0.455 V)[47a] and $[M^{III}(pc)(tpp)]$ (0.465–0.475).[12b] The potentials of all the remaining redox processes also seem to correlate linearly with the metal size (Figure 8), but the effect is weaker, as indicated by the smaller gradients (< 0.5 V Å$^{-1}$). The linear correlation observed between all these potentials and the ionic radius of the central metal indicates that π–π interactions are probably present in these heteroleptic double-deckers, in accord with the spectroscopic data described above.

In comparison with the double-deckers **3** and **5**, the corresponding triple-deckers **15** and **16** undergo oxidations more readily, as shown by the lower oxidation potentials, whereas the first reduction occurs less readily (Table 4). Similarly to the tris(phthalocyaninato)lanthanide(III) complexes $[M^{III}_2\{pc(OC_4H_9)_8\}_3]$ (M = La, Dy, Yb, Lu),[48] the first and second oxidation potentials decrease with the size of the metal center, whereas the reduction processes show only a small metal dependence. All these observations suggest that significant π–π interactions exist in these triple-decker complexes also. The potential differences between the first oxidation and the first reduction are 1.196 and 1.090 V for **15** and **16**, respectively, between those for the homoleptic triple-deckers $[M^{III}_2(oep)_3]$ (M = La, Ce, Eu) (1.81–1.92 V)[49] and $[Lu^{III}_2(1,2\text{-}nc)_3]$ (0.86 V).[20b]

**Absorption spectra of the oxidized and reduced double-deckers**: All the redox processes for the double-deckers involve a one-electron transfer (Scheme 2). The difference between $E_{1/2}$(red1) and $E_{1/2}$(red2) for the neutral complexes **1**–**14** may thus be correlated with the HOMO–LUMO gap of the corresponding reduced species $[M^{III}(nc)(oep)]^-$. The

Table 4. Electrochemical data for **1**–**16**.[a]

| | $E_{1/2}$(oxd4) | $E_{1/2}$(oxd3) | $E_{1/2}$(oxd2) | $E_{1/2}$(oxd1) | $E_{1/2}$(red1) | $E_{1/2}$(red2) |
|---|---|---|---|---|---|---|
| [La(nc)(oep)] (**1**) | | 1.409 | 1.138 | 0.492 | 0.059 | – 1.330 |
| [Pr(nc)(oep)] (**2**) | | 1.361[b] | 1.107[b] | 0.356 | – 0.071 | – 1.416 |
| [Nd(nc)(oep)] (**3**) | | 1.444[b] | 1.198 | 0.407 | – 0.011 | – 1.353 |
| [Sm(nc)(oep)] (**4**) | | 1.380[b] | 1.166 | 0.303 | – 0.122 | – 1.427 |
| [Eu(nc)(oep)] (**5**) | | 1.376[b] | 1.162 [b] | 0.262 | – 0.146 | – 1.432 |
| [Gd(nc)(oep)] (**6**) | | 1.385[b] | 1.158 [b] | 0.246 | – 0.186 | – 1.472[b] |
| [Tb(nc)(oep)] (**7**) | | 1.410[b] | 1.180 | 0.256 | – 0.161 | – 1.440 |
| [Dy(nc)(oep)] (**8**) | | 1.400[b] | 1.177 | 0.230 | – 0.185 | – 1.443 |
| [Y(nc)(oep)] (**9**) | | 1.426[b] | 1.220 | 0.255 | – 0.162 | – 1.411 |
| [Ho(nc)(oep)] (**10**) | | 1.391[b] | 1.178 | 0.192 | – 0.218 | – 1.459 |
| [Er(nc)(oep)] (**11**) | | 1.401 | 1.190 | 0.208 | – 0.207 | – 1.440 |
| [Tm(nc)(oep)] (**12**) | | 1.407 | 1.195 | 0.190 | – 0.201 | – 1.421 |
| [Yb(nc)(oep)] (**13**) | | 1.426[b] | 1.218 | 0.197 | – 0.220 | – 1.451 |
| [Lu(nc)(oep)] (**14**) | | 1.506[b] | 1.293 | 0.255 | – 0.152 | – 1.372[b] |
| $[Nd_2(nc)(oep)_2]$ (**15**) | 1.528[b] | 1.164 | 0.665 | 0.300 | – 0.896[b] | – 1.405 |
| $[Eu_2(nc)(oep)_2]$ (**16**) | 1.563[b] | 1.149 | 0.582 | 0.184 | – 0.906 | – 1.391 |

[a] Recorded with $[Bu_4N][PF_6]$ as electrolyte in $CH_2Cl_2$ (0.1 mol dm$^{-3}$) at ambient temperature. Potentials were obtained by cyclic voltammetry with a scan rate of 100 mV s$^{-1}$, and are expressed as half-wave potentials ($E_{1/2}$) in V relative to SCE unless otherwise stated. [b] By differential pulse voltammetry.

position of the lowest-energy absorption arising from a HOMO–LUMO transition of these anionic complexes can be determined from the general relationship which has been proposed for conjugated π systems [Eq. (1)].[50] The theoret-

$$E_{1/2}(\mathrm{oxd}) - E_{1/2}(\mathrm{red}) - h\nu = 0.01\ \mathrm{eV} \quad (1)$$

ical values are close to the experimental data obtained by adding hydrazine hydrate to solutions of **1**–**14** in $CHCl_3$/MeOH (1:1, *v*/*v*) (Table 5).[51] There is a linear relationship between the blue shift of this near-IR absorption and the size of the metal center with a gradient of approximately $-7\ \mathrm{nm\,pm^{-1}}$ (see Figure S2 in the Supporting information). A similar trend was observed for $[M^{III}(pc)(tpp)]^-$ (M = Y, La, Pr, Nd, Eu, Gd, Er, Lu), in which the lowest-energy Q-band appears at a shorter-wavelength position (746–850 nm).[12b]

Table 5. Comparison between the calculated and experimental values for the lowest-energy absorption band for $[M^{III}(nc)(oep)]^-$ (M = Y, La–Lu except Ce and Pm), **15**, and **16**.

| | $E_{1/2}(\mathrm{oxd}) - E_{1/2}(\mathrm{red})$ [V][a] | $\lambda_{max}$ [nm] calculated[b] | observed[c] |
|---|---|---|---|
| $[La(nc)(oep)]^-$ | 1.389 | 899 | 844 |
| $[Pr(nc)(oep)]^-$ | 1.345 | 929 | 868 |
| $[Nd(nc)(oep)]^-$ | 1.342 | 931 | 878 |
| $[Sm(nc)(oep)]^-$ | 1.305 | 957 | 905 |
| $[Eu(nc)(oep)]^-$ | 1.286 | 972 | 910 |
| $[Gd(nc)(oep)]^-$ | 1.286 | 972 | 920 |
| $[Tb(nc)(oep)]^-$ | 1.279 | 977 | 929 |
| $[Dy(nc)(oep)]^-$ | 1.258 | 994 | 938 |
| $[Y(nc)(oep)]^-$ | 1.249 | 1001 | 944 |
| $[Ho(nc)(oep)]^-$ | 1.241 | 1007 | 948 |
| $[Er(nc)(oep)]^-$ | 1.233 | 1014 | 952 |
| $[Tm(nc)(oep)]^-$ | 1.220 | 1025 | 973 |
| $[Yb(nc)(oep)]^-$ | 1.231 | 1015 | 976 |
| $[Lu(nc)(oep)]^-$ | 1.220 | 1025 | 978 |
| $[Nd_2(nc)(oep)_2]$ (**15**) | 1.196 | 1045 | 1021[d] |
| $[Eu_2(nc)(oep)_2]$ (**16**) | 1.090 | 1148 | 1101[d] |

[a] For the double-decker anions, $E_{1/2}$(red1) and $E_{1/2}$(red2) are taken from Table 4. For the two triple-deckers, the values of $E_{1/2}$(oxd1) and $E_{1/2}$(red1) are used. [b] Calculated according to Equation (1). [c] Measured by adding hydrazine hydrate to $CHCl_3$/MeOH (1:1, *v*/*v*) solutions of the corresponding neutral double-decker complexes, unless otherwise stated. [d] Measured in $CHCl_3$.

The absorption spectra of the double-deckers $[M^{III}(nc)(oep)]^-$ are similar to those of the triple-deckers $[M^{III}_2(nc)(oep)_2]$, which can be regarded as having two $[M^{III}(nc)(oep)]^-$ moieties sharing a common nc ligand.[12a] Accordingly, the unusual near-IR band for the triple-deckers **15** (1021 nm) and **16** (1101 nm) can also be attributed to a HOMO–LUMO transition, or the lowest-energy Q′(0, 0)-band as described above. The assignment is supported by the good agreement between the observed $\lambda_{max}$ and that estimated from the first oxidation and reduction potentials of **15** and **16** (Table 5). In addition, the absorption positions of these two complexes (**16** (1101 nm) > **15** (1021 nm)) are also in line with the trend observed for the anionic double-deckers (Figure S2, Supporting information).

The double-deckers **1**, **5**, and **9** in dichlorobenzene, which contained $[Bu_4N][ClO_4]$ (0.1 mol dm$^{-3}$) as supporting electrolyte, were further investigated by spectroelectrochemical methods, employing a typical thin-layer cell for in situ UV–visible spectroscopic measurements. Their electrochemical behavior in dichlorobenzene was similar to that in $CH_2Cl_2$, but with an additional reduction couple.[52] For example, the spectral changes during the first reduction and oxidation of the $Eu^{III}$ double-decker **5** are displayed in Figure 9, with the absorption spectrum of the neutral complex for comparison. The absorption data for the neutral, singly electro-reduced, and singly electro-oxidized species of the three complexes are summarized in Table 6. Isobestic points are obtained during each electron transfer (Figure 9), showing the lack of spectral intermediates on the thin-layer spectroelectrochemical time-scale. The spectrum for the electro-reduced $[Eu^{III}(nc)(oep)]^-$ is virtually identical to that obtained by chemical reduction by hydrazine hydrate (Table S1, Supporting information). Dur-

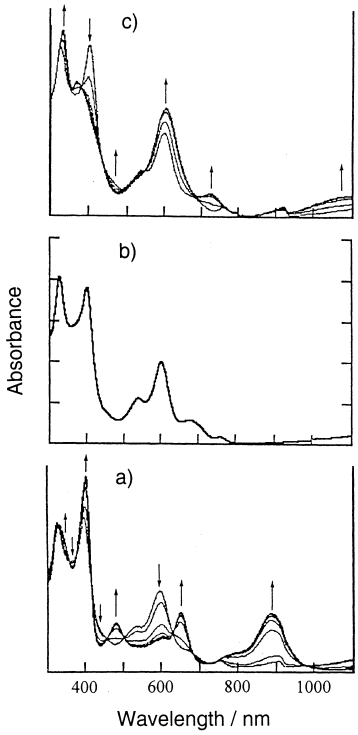


Figure 9. Absorption spectral changes during a) the first electro-reduction and c) the first electro-oxidation of $[Eu^{III}(nc)(oep)]$ (**5**) in dichlorobenzene containing 0.1 mol dm$^{-3}$ $[Bu_4N][ClO_4]$; b) absorption spectrum of neutral $[Eu^{III}(nc)(oep)]$ in $CHCl_3$, for comparison.

Table 6. UV/Vis and near-IR spectroscopic data for the neutral,[a] singly electro-reduced,[b] and singly electro-oxidized[b] species of **1**, **5**, and **9**.

| | $\lambda_{max}$ [nm] | | | | | | | |
|---|---|---|---|---|---|---|---|---|
| $[La(nc)(oep)]^-$ | 330 | 409 | 486 | | 634 | 834 | | |
| $[Eu(nc)(oep)]^-$ | 330 | 404 | 486 | 611 | 654 | 894 | | |
| $[Y(nc)(oep)]^-$ | 334 | 407 | 483 | 612 | 664 | 926 | | |
| $[La(nc)(oep)]$ (**1**) | 327 | 404 | 554 | 612 | 712 | 745 | 1091 | 1816 |
| $[Eu(nc)(oep)]$ (**5**) | 326 | 401 | 539 | 601 | 684 | 757 | 1196 | 1542 |
| $[Y(nc)(oep)]$ (**9**) | 327 | 399 | 530 | 596 | 658 | 772 | 1308 | |
| $[La(nc)(oep)]^+$ | 338 | 385 | | 633 | 773 | | 1400 | |
| $[Eu(nc)(oep)]^+$ | 334 | 370 | | 607 | 723 | | 1095 | |
| $[Y(nc)(oep)]^+$ | 328 | 363 | | 594 | 710 | | 1021 | |

[a] Recorded in $CHCl_3$. [b] Recorded in dichlorobenzene containing 0.1 mol dm$^{-3}$ $[Bu_4N][ClO_4]$.



0947-6539/01/0723-5066 $ 17.50+.50/0 *Chem. Eur. J.* **2001**, *7*, No. 23

ing reduction, the oep B-band increases in intensity and shifts slightly to the red, while the nc B-band remains relatively unchanged (Figure 9a); this indicates that the semi-occupied HOMO may have more oep than nc character. In addition, the diagnostic radical bands at 539 and 1196 nm and the intramolecular ring-to-ring charge transfer band at 1542 nm vanish, while three new bands at 486, 654, and 894 nm that emerge are typical of double-deckers having two dianionic ligands such as $[M^{III}(pc)(tpp)]^-$ (M = Y, La, Pr, Nd, Eu, Gd, Er, Lu),[12] $[M^{III}(pc)(tpyp)]^-$ (M = Eu, Gd),[32a] and $[M^{IV}(pc)(por)]$ (M = Zr, Hf, Th, U; por = oep, tpp).[16]

Figure 9c illustrates the changes that occur upon oxidation of $[Eu^{III}(nc)(oep)]$ to $[Eu^{III}(nc)(oep)]^+$. The nc B-band increases in intensity and is slightly red-shifted, while the reverse trend is observed for the oep B-band giving a blue-shifted signal at 370 nm. The larger spectral changes for the latter may also indicate that the semi-occupied HOMO has a greater contribution from oep than from nc. Whereas there are no significant changes in the visible region, the lowest-energy near-IR absorption is substantially blue-shifted from 1542 to 1095 nm upon oxidation. Similar results have been observed for $[M^{III}(pc)(tpp)]$ (M = Y, La, Pr, Nd, Eu, Gd, Er, Lu)[12b] and $[M^{IV}(por)_2]^+$ (M = Zr, Hf; por = oep, tpp),[53] of which the charge transfer band is blue-shifted by 205–352 and 274–290 nm upon oxidation to the corresponding mono- and dications, respectively. All these observations suggest that each of these species has a di-π-radical character.

The spectroelectrochemical properties of the $La^{III}$ and $Y^{III}$ analogues are similar to those of **5**. The spectral changes are compared in Figure S4 (Supporting information). One of the major differences occurs in the position of the lowest-energy transition, which depends on the size of the metal center. The band shifts slightly to the blue for the anions $[M^{III}(nc)(oep)]^-$, but is substantially red-shifted for the cations $[M^{III}(nc)(oep)]^+$ when the ionic radius increases from $Y^{III}$ to $La^{III}$.

## Conclusion

We have developed a straightforward and simple methodology to prepare a new series of rare earth sandwich complexes with mixed nc and oep ligands. These rare heteroleptic complexes have been fully characterized by a wide range of spectroscopic and electrochemical methods. The molecular structures of four double-deckers and one triple-decker, which represent the first structures reported for nc-containing sandwich complexes, have also been determined. According to the spectroscopic and electrochemical studies, all the complexes exhibit significant π–π interactions. For the double-deckers **1**–**14**, the hole or the unpaired electron is delocalized over both macrocyclic ligands.

## Experimental Section

Purification of solvents, preparation of precursors, spectroscopic measurements, and electrochemical studies have been described in detail elsewhere.[19, 23] The $R_f$ values were measured using $CHCl_3$/hexane (4:1, *v*/*v*) (for all the double-deckers) or toluene (for the two triple-deckers) as eluent. EPR spectra were recorded in $CH_2Cl_2$ at ambient temperature on a Bruker EMX EPR spectrometer equipped with an ER 041 XG microwave bridge (X-band). The field was calibrated using 1,1-diphenyl-2-picrylhydrazyl. The reaction yield, $R_f$ value, spectroscopic (MS, IR, and EPR), and analytical data of all the double-deckers are given in the Supporting information.

**Preparation of 1–14**: A mixture of $[M(acac)_3]\cdot nH_2O$ (0.10 mmol), $H_2$(oep) (27 mg, 0.05 mmol), naphthalonitrile (72 mg, 0.40 mmol), and 1,8-diazabicyclo[5.4.0]undec-7-ene (DBU; 0.05 mL, 0.33 mmol) in *n*-octanol (4 mL) was refluxed overnight (>18 h) under nitrogen to give a dark green solution. The solvent was removed under reduced pressure, and the residue was purified by chromatography on a silica gel column with $CH_2Cl_2$/hexane (1:1, *v*/*v*) as eluent. Part of the unreacted metal-free porphyrin was collected as the first fraction. The column was then eluted successively with $CH_2Cl_2$, $CHCl_3$, and MeOH in $CHCl_3$ (3%) to give the desired double-decker, which was contaminated with a small amount of $H_2$(oep) as shown by UV/Vis spectroscopy. The crude product was further purified by repetition of the same chromatographic procedure, followed by recrystallization from a mixture of $CHCl_3$ and MeOH to afford dark blue microcrystals.

**Preparation of 15 and 16**: A mixture of $[M^{III}(nc)(oep)]$ [M = Nd (**3**), Eu (**5**)] (16 μmol), $H_2$(oep) (14 mg, 26 μmol), and $[M(acac)_3]\cdot nH_2O$ (M = Nd, Eu) (0.05 mmol) in 1,2,4-trichlorobenzene (TCB; 4 mL) was refluxed under nitrogen for 18 h to give a greenish blue solution. The solvent was removed under reduced pressure, and the residue was subjected to chromatography on a silica gel column with $CH_2Cl_2$/hexane (1:1, *v*/*v*) as eluent to remove the unreacted $[M^{III}(nc)(oep)]$ and $H_2$(oep). The column was then eluted with toluene to develop a green band containing $[M^{III}_2(nc)(oep)_2]$, which was purified by repeated chromatography followed by recrystallization from a mixture of $CHCl_3$ and MeOH.

**$[Nd_2(nc)(oep)_2]$ (15)**: Yield 15 mg (46%); $R_f = 0.78$; $^1$H NMR (300 MHz, [D$_5$]pyridine): $\delta = 7.53$ (br s, 8H; *meso*-H or nc-H), 7.29 (br s, 8H; *meso*-H or nc-H), 5.91 (br s, 8H; *meso*-H or nc-H), 3.79 (br s, 8H; *meso*-H or nc-H), 2.60–2.72 (m, 16H; $CH_2$), 1.20–1.40 (m, 16H; $CH_2$), 0.78–0.96 (m, 48H; $CH_3$); MS (MALDI-TOF): *m*/*z*: 2064 $[M]^+$; elemental analysis calcd (%) for $C_{121}H_{113}Cl_3N_{16}Nd_2$ (**15**·$CHCl_3$) (2186.2): C 66.48, H 5.21, N 10.25; found: C 66.63, H 5.47, N 9.90.

**$[Eu_2(nc)(oep)_2]$ (16)**: Yield 21 mg (63%); $R_f = 0.84$; $^1$H NMR (300 MHz, [D$_5$]pyridine): $\delta = 13.52$ (br s, 8H; nc-H$_\alpha$), 13.16 (br s, 8H; *meso*-H), 10.66–10.74 (m, 8H; nc-H$_\beta$), 9.20–9.30 (m, 8H; nc-H$_\gamma$), 4.70–4.82 (m, 16H; $CH_2$), 3.12–3.28 (m, 16H; $CH_2$), 1.14–1.28 (m, 48H; $CH_3$); MS (MALDI-TOF): *m*/*z*: 2081 $[M]^+$; elemental analysis calcd (%) for $C_{122.5}H_{114.5}Cl_{75}Eu_2N_{16}$ (**16**·2.5$CHCl_3$) (2380.7): C 61.80, H 4.85, N 9.41; found: C 61.94, H 4.97, N 8.95.

**X-ray crystallographic analyses of 4, 6, 9, 14, and 15**: Crystal data and details of data collection and structure refinement are given in Table 7. Data were collected on a Bruker SMART CCD diffractometer with an $Mo_{K\alpha}$ sealed tube ($\lambda = 0.71073$ Å) at 293 K, and by using a ω scan mode with an increment of 0.3°. Preliminary unit cell parameters were obtained from 45 frames. Final unit cell parameters were derived by global refinements of reflections obtained from integration of all the frame data. The collected frames were integrated by using the preliminary cell-orientation matrix. SMART software was used for collecting frames of data, indexing reflections, and determination of lattice constants; SAINT-PLUS for integration of intensity of reflections and scaling;[54] SADABS for absorption correction;[55] and SHELXL for space group and structure determination, refinements, graphics, and structure reporting.[56] Crystallographic data (excluding structure factors) for the structures reported in this paper have been deposited with the Cambridge Crystallographic Data Centre as supplementary publication no. CCDC-165147–165151. Copies of the data can be obtained free of charge on application to CCDC, 12 Union Road, Cambridge CB2 1EZ, UK (fax: (+44) 1223-336-033; e-mail: deposit@ccdc.cam.ac.uk).

## Acknowledgements

We thank Prof. Hung-Kay Lee for recording the EPR spectra. Financial support from the Natural Science Foundation of China (Grant No. Z017102); the State Educational Ministry of China; the Natural Science Foundation of Shandong Province (Grant No. Z99B03); the Science Committee of Shandong Province; Shandong University; the State

Table 7. Crystallographic data for **4**, **6**, **9**, **14**, and **15**.

| | **4** · 0.5 $C_6H_{12}$ | **6** | **9** · 0.5 $C_6H_{12}$ | **14** | **15** · $CH_2Cl_2$ · 2 $H_2O$ |
|---|---|---|---|---|---|
| formula | $C_{87}H_{74}N_{12}Sm$ | $C_{84}H_{68}GdN_{12}$ | $C_{87}H_{74}N_{12}Y$ | $C_{84}H_{68}LuN_{12}$ | $C_{121}H_{118}Cl_2N_{16}Nd_2O_2$ |
| $M_r$ | 1437.9 | 1402.8 | 1376.5 | 1420.5 | 2187.7 |
| crystal size [$mm^3$] | 0.77 × 0.20 × 0.06 | 0.46 × 0.40 × 0.13 | 0.39 × 0.24 × 0.06 | 0.55 × 0.35 × 0.14 | 0.55 × 0.22 × 0.08 |
| crystal system | orthorhombic | orthorhombic | orthorhombic | orthorhombic | orthorhombic |
| space group | *Pna2₁* | *Pna2₁* | *Pna2₁* | *Pna2₁* | *Pccn* |
| *a* [Å] | 28.8000 (12) | 28.708 (6) | 28.7098 (12) | 28.9566 (12) | 24.826 (1) |
| *b* [Å] | 10.9682 (4) | 10.951 (2) | 10.9279 (5) | 10.9212 (4) | 28.057 (2) |
| *c* [Å] | 26.5153 (11) | 26.524 (5) | 26.5642 (12) | 26.9686 (11) | 16.623 (1) |
| *V* [$Å^3$] | 8375.8 (6) | 8339 (3) | 8334.2 (6) | 8528.6 (6) | 11578 (1) |
| *Z* | 4 | 4 | 4 | 4 | 4 |
| *F*(000) | 2984 | 2880 | 2892 | 2908 | 4504 |
| $\rho_{calcd}$ [$Mg\,m^{-3}$] | 1.144 | 1.117 | 1.100 | 1.106 | 1.255 |
| $\mu$ [$mm^{-1}$] | 0.749 | 0.842 | 0.748 | 1.203 | 0.988 |
| $\theta$ range [°] | 1.41 – 24.00 | 2.34 – 24.00 | 1.42 – 24.00 | 1.41 – 24.00 | 1.64 – 24.00 |
| reflections collected | 41430 | 16651 | 40782 | 41766 | 56781 |
| independent reflections | 10958 ($R_{int}$ = 0.0918) | 5864 ($R_{int}$ = 0.1477) | 12514 ($R_{int}$ = 0.1347) | 12748 ($R_{int}$ = 0.0570) | 9035 ($R_{int}$ = 0.0886) |
| parameters | 864 | 850 | 899 | 846 | 667 |
| *R*1 [$I > 2\sigma(I)$] | 0.0556 | 0.0839 | 0.0633 | 0.0426 | 0.0559 |
| w*R*2 [$I > 2\sigma(I)$] | 0.1343 | 0.1972 | 0.1508 | 0.1079 | 0.1667 |
| goodness of fit | 1.024 | 1.077 | 0.884 | 1.001 | 0.988 |

Key Laboratory of Rare Earths at Peking University; the Ministry of Education, Science, Sports, and Culture of Japan (Grant-in-Aid for Scientific Research on Priority Area "Creation of Delocalized Electron Systems" No. 11133206); and the Chinese University of Hong Kong is gratefully acknowledged.

[1] a) *Phthalocyanines—Properties and Applications*, *Vols. 1–4* (Eds.: C. C. Leznoff, A. B. P. Lever), VCH, New York, **1989–1996**; b) N. B. McKeown, *Phthalocyanine Materials—Synthesis, Structure and Function*, Cambridge University Press, New York, **1998**.

[2] *The Porphyrin Handbook*, *Vols. 1–10* (Eds.: K. M. Kadish, K. M. Smith, R. Guilard), Academic Press, San Diego, **2000**.

[3] a) J. W. Buchler, D. K. P. Ng in *The Porphyrin Handbook*, *Vol. 3* (Eds.: K. M. Kadish, K. M. Smith, R. Guilard), Academic Press, San Diego, **2000**, pp. 245–294; b) J. Jiang, K. Kasuga, D. P. Arnold in *Supramolecular Photo-sensitive and Electro-active Materials* (Ed.: H. S. Nalwa), Academic Press, New York, **2001**, pp. 113–210.

[4] M. M. Nicholson in *Phthalocyanines—Properties and Applications*, *Vol. 3* (Eds.: C. C. Leznoff, A. B. P. Lever), VCH, New York, **1993**, pp. 71–117.

[5] a) M. Madru, G. Guillaud, M. Al Sadoun, M. Maitrot, C. Clarisse, M. Le Contellec, J.-J. André, J. Simon, *Chem. Phys. Lett.* **1987**, *142*, 103; b) R. Madru, G. Guillaud, M. Al Sadoun, M. Maitrot, J.-J. André, J. Simon, R. Even, *Chem. Phys. Lett.* **1988**, *145*, 343; c) C. Clarisse, M. T. Riou, M. Gauneau, M. Le Contellec, *Electron. Lett.* **1988**, *24*, 674; d) G. Guillaud, M. Al Sadoun, M. Maitrot, J. Simon, M. Bouvet, *Chem. Phys. Lett.* **1990**, *167*, 503.

[6] a) J. Souto, M. L. Rodríguez, J. A. Desaja, R. Aroca, *Int. J. Electron.* **1994**, *76*, 763; b) P. Bassoul, T. Toupance, J. Simon, *Sens. Actuators B* **1995**, *26–27*, 150; c) K. R. Rickwood, D. R. Lovett, B. Lukas, J. Silver, *J. Mater. Chem.* **1995**, *5*, 725; d) B. Liang, C. Yuan, Y. Wei, Y. Zhang, D. Jiang, S. Zhang, A. Lu, *Synth. Met.* **1997**, *88*, 219; e) J. Álvarez, J. Souto, M. L. Rodríguez-Méndez, J. A. de Saja, *Sens. Actuators B* **1998**, *48*, 339.

[7] a) J. W. Buchler, K. Elsässer, M. Kihn-Botulinski, B. Scharbert, *Angew. Chem.* **1986**, *98*, 257; *Angew. Chem. Int. Ed. Engl.* **1986**, *25*, 286; b) J. W. Buchler, *Comments Inorg. Chem.* **1987**, *6*, 175.

[8] a) A. Sugasaki, M. Ikeda, M. Takeuchi, A. Robertson, S. Shinkai, *J. Chem. Soc. Perkin Trans. 1* **1999**, 3259; b) A. Sugasaki, M. Ikeda, M. Takeuchi, S. Shinkai, *Angew. Chem.* **2000**, *112*, 3997; *Angew. Chem. Int. Ed.* **2000**, *39*, 3839; c) A. Sugasaki, M. Ikeda, M. Takeuchi, K. Koumoto, S. Shinkai, *Tetrahedron* **2000**, *56*, 4717.

[9] K. Tashiro, K. Konishi, T. Aida, *J. Am. Chem. Soc.* **2000**, *122*, 7921.

[10] D. K. P. Ng, J. Jiang, *Chem. Soc. Rev.* **1997**, *26*, 433.

[11] Abbreviations used for tetrapyrrole derivatives: nc = 2,3-naphthalocyaninate; nc(*t*Bu)$_4$ = tetra(*tert*-butyl)-2,3-naphthalocyaninate; nc($SC_{12}H_{25}$)$_8$ = 3,4,12,13,21,22,30,31-octakis(dodecylthio)-2,3-naphthalocyaninate; oep = octaethylporphyrinate; pc = phthalocyaninate; pc(OR)$_8$ = 2,3,9,10,16,17,23,24-octaalkoxyphthalocyaninate; por = general porphyrinate; tbpp = *meso*-tetrakis(4-*tert*-butylphenyl)-porphyrinate; tClpp = *meso*-tetrakis(4-chlorophenyl)porphyrinate; tpp = *meso*-tetraphenylporphyrinate; tpyp = *meso*-tetra(4-pyridyl)-porphyrinate.

[12] a) T.-H. Tran-Thi, T. A. Mattioli, D. Chabach, A. De Cian, R. Weiss, *J. Phys. Chem.* **1994**, *98*, 8279; b) D. Chabach, M. Tahiri, A. De Cian, J. Fischer, R. Weiss, M. El Malouli Bibout, *J. Am. Chem. Soc.* **1995**, *117*, 8548.

[13] J. W. Buchler, J. Löffler, *Z. Naturforsch*, *Teil B* **1990**, *45*, 531.

[14] a) J. W. Buchler, A. De Cian, J. Fischer, P. Hammerschmitt, J. Löffler, B. Scharbert, R. Weiss, *Chem. Ber.* **1989**, *122*, 2219; b) J. K. Duchowski, D. F. Bocian, *Inorg. Chem.* **1990**, *29*, 4158.

[15] G. S. Girolami, P. A. Gorlin, S. N. Milam, K. S. Suslick, S. R. Wilson, *J. Coord. Chem.* **1994**, *32*, 173.

[16] a) K. M. Kadish, G. Moninot, Y. Hu, D. Dubois, A. Ibnlfassi, J.-M. Barbe, R. Guilard, *J. Am. Chem. Soc.* **1993**, *115*, 8153; b) R. Guilard, J.-M. Barbe, A. Ibnlfassi, A. Zrineh, V. A. Adamian, K. M. Kadish, *Inorg. Chem.* **1995**, *34*, 1472.

[17] a) E. Ortí, M. C. Piqueras, R. Crespo, J. L. Brédas, *Chem. Mater.* **1990**, *2*, 110; b) E. Ortí, R. Crespo, M. C. Piqueras, J. L. Brédas, *Synth. Met.* **1991**, *41–43*, 2647; c) E. Ortí, R. Crespo, M. C. Piqueras, F. Tomás, *J. Mater. Chem.* **1996**, *6*, 1751.

[18] F. Guyon, A. Pondaven, P. Guenot, M. L'Her, *Inorg. Chem.* **1994**, *33*, 4787.

[19] a) J. Jiang, W. Liu, K.-W. Poon, D. Du, D. P. Arnold, D. K. P. Ng, *Eur. J. Inorg. Chem.* **2000**, 205; b) T. Nyokong, F. Furuya, N. Kobayashi, D. Du, W. Liu, J. Jiang, *Inorg. Chem.* **2000**, *39*, 128.

[20] a) F. Guyon, A. Pondaven, M. L'Her, *J. Chem. Soc. Chem. Commun.* **1994**, 1125; b) F. Guyon, A. Pondaven, J.-M. Kerbaol, M. L'Her, *Inorg. Chem.* **1998**, *37*, 569.

[21] Prior to our work, only one heteroleptic naphthalocyaninato complex, [$Lu^{III}$(nc)(pc)], had been reported. See: a) M. Bouvet, J. Simon, *Chem. Phys. Lett.* **1990**, *172*, 299; b) N. Ishikawa, O. Ohno, Y. Kaizu, *Chem. Phys. Lett.* **1991**, *180*, 51; c) N. Ishikawa, O. Ohno, Y. Kaizu, *J. Phys. Chem.* **1993**, *97*, 1004; d) M. Bouvet, P. Bassoul, J. Simon, *Mol. Cryst. Liq. Cryst.* **1994**, *252*, 31; e) M. Passard, J. P. Blanc, C. Maleysson, *Thin Solid Films* **1995**, *271*, 8; f) M. Passard, A. Pauly, J. P. Germain, C. Maleysson, *Synth. Met.* **1996**, *80*, 25; g) V. N. Nemykin, S. V. Volkov, *Russ. J. Coord. Chem.* **2000**, *26*, 436; Simon and co-workers have very recently reported the 1,2-naphthalocyaninato analogue [$Lu^{III}$(1,2-nc)(pc)] as a mixture of structural and/or

  0947-6539/01/0723-5068 $ 17.50+.50/0 

optical isomers, in: h) V. M. Negrimovskii, M. Bouvet, E. A. Luk'yanets, J. Simon, *J. Porphyrins Phthalocyanines* **2001**, *5*, 423.
[22] J. Jiang, D. Du, M. T. M. Choi, J. Xie, D. K. P. Ng, *Chem. Lett.* **1999**, 261.
[23] J. Jiang, W. Liu, K.-L. Cheng, K.-W. Poon, D. K. P. Ng, *Eur. J. Inorg. Chem.* **2001**, 413.
[24] Under similar conditions, $[Ce(acac)_3]\cdot nH_2O$ was converted to the $Ce^{IV}$ double-decker $[Ce^{IV}(nc)(oep)]$, which has properties that are very different from those of the $M^{III}$ counterparts. This compound, together with a series of other $Ce^{III/IV}$ double-deckers, will be reported elsewhere.
[25] J. W. Buchler, J. Hüttermann, J. Löffler, *Bull. Chem. Soc. Jpn.* **1988**, *61*, 71.
[26] D. Chabach, A. De Cian, J. Fischer, R. Weiss, M. El Malouli Bibout, *Angew. Chem.* **1996**, *108*, 942; *Angew. Chem. Int. Ed. Engl.* **1996**, *35*, 898.
[27] No attempts were made to prepare other lanthanide triple-deckers $[M^{III}_2(nc)(oep)_2]$, but it is expected that they can be prepared similarly, at least for those lanthanides comparable in size with the $Nd^{III}$ and $Eu^{III}$ ions.
[28] R. L. C. Lau, J. Jiang, D. K. P. Ng, T.-W. D. Chan, *J. Am. Soc. Mass Spectrom.* **1997**, *8*, 161.
[29] a) A. Pondaven, Y. Cozien, M. L'Her, *New J. Chem.* **1992**, *16*, 711; b) C. Cadiou, A. Pondaven, M. L'Her, P. Jehan, P. Guenot, *J. Org. Chem.* **1999**, *64*, 9046.
[30] The difficulty in interpreting the $^1H$ NMR spectra for the other rare earth double-deckers could be related to the different magnetic properties of the metal ions.
[31] Two multiplets for the diastereotopic methylene protons were also observed for other oep-containing double- and triple-decker complexes. See, for example: a) J. W. Buchler, A. De Cian, J. Fischer, M. Kihn-Botulinski, H. Paulus, R. Weiss, *J. Am. Chem. Soc.* **1986**, *108*, 3652; b) J. W. Buchler, M. Kihn-Botulinski, J. Löffler, M. Wicholas, *Inorg. Chem.* **1989**, *28*, 3770; c) J. P. Collman, J. L. Kendall, J. L. Chen, T. A. Eberspacher, C. R. Moylan, *Inorg. Chem.* **1997**, *36*, 5603.
[32] a) J. Jiang, T. C. W. Mak, D. K. P. Ng, *Chem. Ber.* **1996**, *129*, 933; b) J. Jiang, M. T. M. Choi, W.-F. Law, J. Chen, D. K. P. Ng, *Polyhedron* **1998**, *17*, 3903; c) J. Jiang, J. Xie, M. T. M. Choi, Y. Yan, S. Sun, D. K. P. Ng, *J. Porphyrins Phthalocyanines* **1999**, *3*, 322.
[33] a) J. W. Buchler, M. Knoff in *Optical Properties and Structure of Tetrapyrroles* (Eds.: G. Blauer, H. Sund), de Gruyter, Berlin, **1985**, pp. 91–105; b) J. W. Buchler, K. Elsässer, M. Kihn-Botulinski, B. Scharbert, S. Tansil, *ACS Symp. Ser.* **1986**, *321*, 94.
[34] a) J. K. Duchowski, D. F. Bocian, *J. Am. Chem. Soc.* **1990**, *112*, 3312; b) O. Bilsel, J. Rodriguez, S. N. Milam, P. A. Gorlin, G. S. Girolami, K. S. Suslick, D. Holten, *J. Am. Chem. Soc.* **1992**, *114*, 6528.
[35] This characteristic near-IR band can also be simply assigned to an intramolecular ring-to-ring charge transfer transition on the assumption that the hole resides mainly on one of the macrocyclic ligands. See refs. [3] and [10].
[36] L. L. Wittmer, D. Holten, *J. Phys. Chem.* **1996**, *100*, 860.
[37] J. Jiang, X. Sun, X. Cui, D. P. Arnold, M. T. M. Choi, D. K. P. Ng, unpublished results.
[38] a) J. Jiang, R. L. C. Lau, T. W. D. Chan, T. C. W. Mak, D. K. P. Ng, *Inorg. Chim. Acta* **1997**, *255*, 59; b) J. Jiang, W. Liu, W.-F. Law, D. K. P. Ng, *Inorg. Chim. Acta* **1998**, *268*, 49.
[39] Although such a near-IR absorption was observed previously for $[M^{III}_2(pc)(tpp)_2]$ (M = Ce, Gd) and $[Ce^{III}_2\{pc(OMe)_8\}(tpp)_2]$ at approximately 890 nm, the origin of this band was not discussed. See: a) ref. [12a]; b) D. Chabach, M. Lachkar, A. De Cian, J. Fischer, R. Weiss, *New J. Chem.* **1992**, *16*, 431.
[40] a) J. Jiang, D. P. Arnold, H. Yu, *Polyhedron* **1999**, *18*, 2129; b) J. Jiang, L. Rintoul, D. P. Arnold, *Polyhedron* **2000**, *19*, 1381; c) J. Jiang, U. Cornelissen, D. P. Arnold, X. Sun, H. Homborg, *Polyhedron* **2001**, *20*, 557.
[41] The differences between the first oxidation potentials of $[M^{III}(oep)_2]$ and those of the respective $[M^{III}\{nc(t\text{Bu})_4\}_2]$ are less than 0.1 V. See: a) ref. [19a]; b) J. W. Buchler, B. Scharbert, *J. Am. Chem. Soc.* **1988**, *110*, 4272.
[42] Due to the lower solubility of **15** in $CHCl_3$, other solvents including toluene, THF, and $CH_2Cl_2$ were added to dissolve the complex completely.
[43] Gas chromatography showed that the hexane we used contained approximately 1% of cyclohexane.
[44] N. Koike, H. Uekusa, Y. Ohashi, C. Harnoode, F. Kitamura, T. Ohsaka, K. Tokuda, *Inorg. Chem.* **1996**, *35*, 5798.
[45] Homborg and co-workers have recently reported the structures of 14 $[M(pc)_2]^-$ complexes and found that the twist angles do not simply depend inversely on the interplanar distance as reported by Ohashi and co-workers (ref. [44]). Owing to the small energy difference between the cubic (twist angle = 0°) and the square anti-prismatic (twist angle = 45°) conformations, other factors such as the cation–anion interactions and the effects of solvated molecules may also play a dominant role. See: H. Hückstädt, A. Tutaß, M. Göldner, U. Cornelissen, H. Homborg, *Z. Anorg. Allg. Chem.* **2001**, *627*, 485.
[46] A plot of potentials of these five one-electron transfer processes versus the ring-to-ring separation for **4**, **6**, **9**, and **14**, of which the structural data are available, shows a similar trend (see Figure S1 in the Supporting information).
[47] a) H. Konami, M. Hatano, N. Kobayashi, T. Osa, *Chem. Phys. Lett.* **1990**, *165*, 397; b) J. W. Buchler, P. Hammerschmitt, I. Kaufeld, J. Löffler, *Chem. Ber.* **1991**, *124*, 2151; c) A. Iwase, C. Harnoode, Y. Kameda, *J. Alloys Compd.* **1993**, *192*, 280.
[48] K. Takahashi, M. Itoh, Y. Tomita, K. Nojima, K. Kasuga, K. Isa, *Chem. Lett.* **1993**, 1915; b) K. Takahashi, J.-i. Shimoda, M. Itoh, Y. Fuchita, H. Okawa, *Chem. Lett.* **1998**, 173.
[49] J. K. Duchowski, D. F. Bocian, *J. Am. Chem. Soc.* **1990**, *112*, 8807.
[50] J.-H. Fuhrhop, K. M. Kadish, D. G. Davis, *J. Am. Chem. Soc.* **1973**, *95*, 5140.
[51] The calculated and experimental $\lambda_{max}$ values differ by 39–62 nm. The other absorption data for $[M^{III}(nc)(oep)]^-$ are given in Table S1 as Supporting information.
[52] A typical cyclic voltammogram and differential pulse voltammogram for **5** (Figure S3), together with the electrochemical data for **1**, **5**, and **9** in dichlorobenzene (Table S2) are given as Supporting information.
[53] J. W. Buchler, A. De Cian, S. Elschner, J. Fischer, P. Hammerschmitt, R. Weiss, *Chem. Ber.* **1992**, *125*, 107.
[54] SMART and SAINT for Windows NT Software Reference Manuals, Version 5.0, Bruker Analytical X-Ray Systems, Madison, WI, **1997**.
[55] G. M. Sheldrick, SADABS—A Software for Empirical Absorption Correction, University of Göttingen, Germany, **1997**.
[56] SHELXL Reference Manual, Version 5.1, Bruker Analytical X-Ray Systems, Madison, WI, **1997**.
[57] R. D. Shannon, *Acta Crystallogr. Sect. A* **1976**, *32*, 751; the effective ionic radii of the octacoordinate metal ions were taken.

Received: June 15, 2001 [F3336]